

Kenngottite, $\text{Mn}_3^{2+}\text{Fe}_4^{3+}(\text{PO}_4)_4(\text{OH})_6(\text{H}_2\text{O})_2$: a new phosphate mineral from Krásno near Horní Slavkov, Czech Republic

Jiří SEJKORA^{1,*}, IAN E. GREY² and ANTHONY R. KAMPF³

¹Department of Mineralogy and Petrology, National Museum, Cirkusová 1740, 193 00 Praha 9, Czech Republic

*Corresponding author, e-mail: jiri_sejkora@nm.cz

²CSIRO Mineral Resources, Private Bag 10, Clayton South, Victoria 3169, Australia

³Mineral Sciences Department, Natural History Museum of Los Angeles County, 900 Exposition Boulevard, Los Angeles, CA 90007, USA

Abstract: Kenngottite, $\text{Mn}_3^{2+}\text{Fe}_4^{3+}(\text{PO}_4)_4(\text{OH})_6(\text{H}_2\text{O})_2$, is a new phosphate mineral from the Krásno ore district near Horní Slavkov, Czech Republic. It occurs in association with phosphosiderite, fluorapatite, Mn-rich dufrénite, frondelite, rockbridgeite, morinite, beraunite, strengite, natrodufrénite, fluorite and a K–Mn oxide. It forms brown aggregates up to 3 mm across in tiny cavities of hydrothermally altered black rockbridgeite-group minerals. These aggregates are composed of imperfect laths to fibrous crystals up to 0.5 mm in size. Kenngottite has a light brown streak and a vitreous to pearly lustre. It does not fluoresce under either short- or long-wave ultraviolet light. Its aggregates are opaque; individual crystals or tiny fragments are translucent to transparent. Cleavage is not directly observed, probably parallel to {100}, the Mohs hardness is ~4–5 (by analogy with souzalite and gormanite), and the mineral is brittle with an uneven, stepped fracture. The calculated density is 3.40 g/cm³. Kenngottite is optically biaxial positive, the indices of refraction are $\alpha = 1.785(1)$, $\beta = 1.790(5)$, $\gamma = 1.810(2)$, and $2V_{\text{meas.}}$ is $50(10)^\circ$. Kenngottite is monoclinic, space group $P2_1/a$, $a = 13.909(10)$, $b = 5.186(4)$, $c = 12.159(9)$ Å, $\beta = 98.88(1)^\circ$, $V = 866.5(11)$ Å³, $Z = 2$. The eight strongest lines in the X-ray powder diffraction pattern are as follows: d (Å)/ hkl : 4.87/47(20 $\bar{2}$,110); 3.458/89(40 $\bar{1}$,310); 3.209/100(203,311,11 $\bar{3}$,013,31 $\bar{2}$); 3.023/31(113,004); 2.623/46(114,204,020); 2.429/49(510,220,314); 1.9506/28(024,224) and 1.5772/34(624). The chemical analyses by electron microprobe yielded (in wt%) Na₂O 0.03, MnO 17.82, CaO 0.31, ZnO 0.32, Fe₂O₃ 35.30, Al₂O₃ 2.71, P₂O₅ 30.80, As₂O₅ 0.15, SiO₂ 0.08, H₂O_{calc.} 9.60, total 97.12. The resulting empirical formula on the basis of 24 O atoms per formula unit (*apfu*) is $(\text{Mn}_{2.29}\text{Fe}_{0.53}\text{Ca}_{0.05}\text{Zn}_{0.04}\text{Na}_{0.01})_{\Sigma 2.92}(\text{Fe}_{3.51}\text{Al}_{0.49})_{\Sigma 4.00}[(\text{PO}_4)_{3.96}(\text{AsO}_4)_{0.01}(\text{SiO}_4)_{0.01}]_{\Sigma 3.98}(\text{OH})_{6.42}(\text{H}_2\text{O})_{1.66}$. The crystal structure of kenngottite was solved using single-crystal X-ray diffraction data and refined to $wR_{\text{obs}} = 0.088$ for 350 reflections with $I > 2\sigma(I)$. The structure contains trimeric clusters of face-shared octahedra (Mn–Fe–Mn) that are connected into chains along [001] by sharing edges with Mn-centred octahedra. The chains are corner-connected along [100] to linear corner-shared trimers of Fe-centred octahedra and along [010] *via* corner-connected PO₄ tetrahedra. Monoclinic kenngottite is structurally related to triclinic souzalite and gormanite. It is named in honor of the prominent mineralogist Prof. Gustav Adolf Kenngott (1818–1897) from the University of Zürich (Switzerland) for his contributions to systematic mineralogy.

Key-words: kenngottite; new mineral; phosphate; manganese iron phosphate hydroxyhydrate; crystal structure; Raman spectroscopy; Krásno near Horní Slavkov; Czech Republic.

1. Introduction

During our investigations of late hydrothermal and supergene F-rich phosphate assemblages from Krásno ore district, Czech Republic, a number of rare and unusual minerals have been discovered (Sejkora *et al.*, 2006a, b). One of this suite was a probably new Fe–Mn phosphate described as an unnamed mineral phase *UNK9* by Sejkora *et al.* (2006c) with X-ray powder diffraction data and chemical composition close to those published for the unnamed Fe–Mn “dufrénite-like” mineral from Buranga, Rwanda, by von Knorring & Sahama (1982). New investigations (including a determination of the crystal structure) revealed this mineral to be structurally related to souzalite and gormanite and provided the ideal formula $\text{Mn}_3^{2+}\text{Fe}_4^{3+}(\text{PO}_4)_4(\text{OH})_6(\text{H}_2\text{O})_2$.

The new mineral is named kenngottite in honour of the prominent mineralogist Prof. Gustav Adolf Kenngott (1818–1897) from the University of Zürich (Switzerland) for his contributions to systematic mineralogy. Prof. Kenngott was an author of a series of successful colour-plate mineralogy books and also published the description of the first new mineral from Krásno, carpholite (Kenngott, 1851). The name kenngottite was used in the past as a synonym for plumboan miargyrite (Haidinger, 1856 in Palache *et al.*, 1944) or as a name for the amorphous variety of arsenolite (de Fourestier, 1999). Both invalid names have not been used for more than 50 years.

The new mineral and name have been approved by the Commission on New Minerals, Nomenclature and Classification of the International Mineralogical Association

(IMA 2018-063). The holotype specimen is deposited in the collections of the Department of Mineralogy and Petrology of the National Museum in Prague, Cirkusová 1740, Praha 9, Czech Republic, catalogue number P1P 26/2018. Crystals from the holotype are deposited as a cotype in the collections of the Natural History Museum of Los Angeles County, 900 Exposition Boulevard, Los Angeles, CA 90007, USA, catalogue number 66795.

2. Occurrence

Kenngottite occurs at the Krásno ore district near Horní Slavkov, Slavkovský les area, Czech Republic. The Krásno ore district belongs to one of the most important areas of tin and tungsten mining in central Europe (Beran & Sejkora, 2006). The district is represented by greisen mineralization in several granite cupolas of the large Krušné hory (Erzgebirge) granite batholith underlying metamorphic rock (mainly gneisses). The largest Sn–W deposit in this district is the Huber stock. In the past, it was mined *via* the Huber open pit and Huber (Stannum) shaft down to 200 m under the surface (5th level at 425 m a.s.l.). The stock is bell-shaped in section, similar to a blunt cone. At 100 m beneath the present surface, the stock is 200 × 100 m in cross-section, while at 150 m beneath the surface, the stock extends NE–SW and is about 400 × 250 m in cross section. The Huber stock consists of autometamorphosed Li-mica–topaz granite with a variable degree of greisenization. It is assumed that the entire apical part of this cupola was formed by greisen and quartz with rich ore mineralization (Beran & Sejkora, 2006). Detailed descriptions of the mineralogy (more than 230 mineral species) of the Krásno ore district were published by Beran & Sejkora (2006) and Sejkora *et al.* (2006a–c). More recently, the new minerals tvrdýite (Sejkora *et al.*, 2016), krásnoite (Mills *et al.*, 2012), and iangreyite (Mills *et al.*, 2011) were described from this locality, which also hosts the second world occurrences of kunatite (Mills *et al.*, 2008) and plimerite (Sejkora *et al.*, 2011).

Kenngottite samples were found at the 5th level of the Huber shaft (50°07'22"N 12°48'2"E), at the well documented phosphate accumulation (Sejkora *et al.*, 2006b). This accumulation consists of dominant fluorapatite and triplite aggregates from 10 cm to 1 m in size, located in coarse-grained white quartz in the Huber stock. Aggregates of dark Fe–Mn phosphates with predominant frondelite occur along contacts of these phosphate accumulations with white quartz and cavernous corroded portions carrying younger phosphates (iangreyite, strengite and minerals of the chalcocyanite–turquoise series). Kenngottite from Krásno was originally described as an unnamed mineral phase *UNK9* by Sejkora *et al.* (2006c).

The new mineral kenngottite is intergrown with phosphosiderite, fluorapatite and Mn-rich dufrénite in association with rockbridgeite-group minerals (rockbridgeite–frondelite) and relics of triplite in quartz gangue (holotype sample). In other samples, microscopic aggregates of kenngottite were observed in association with morinite, beraunite, strengite, natrodufrénite, fluorite and a K–Mn oxide.

3. Morphology, physical properties and optical data

Kenngottite occurs as brown aggregates (Fig. 1) in tiny cavities of hydrothermally altered black rockbridgeite-group minerals (rockbridgeite–frondelite) which have nearly completely replaced earlier triplite. Tabular aggregates up to 3 mm across are composed of imperfect laths to fibrous crystals probably elongated along [010] and flattened on {100}, up to 0.5 mm in size (Figs. 2 and 3). Kenngottite has a light to dark brown colour. Its aggregates are opaque; individual crystals or tiny fragments are translucent to transparent. It has a light brown streak and a vitreous to pearly lustre. It does not fluoresce under either short- or long-wave ultraviolet light. Cleavage is not directly observed, probably parallel to {100}, the Mohs hardness is ~4–5 (by analogy with souzalite and gormanite), and the mineral is brittle with an uneven, stepped fracture. The density could not be measured because of the small size of crystals and their intergrowths with other minerals. The density $D_{\text{calc}} = 3.40 \text{ g/cm}^3$ was calculated on the basis of the empirical formula and unit-cell volume from the single-crystal data; for the ideal formula, the calculated density is 3.47 g cm^{-3} .

Kenngottite is optically biaxial positive, with $\alpha = 1.785(1)$, $\beta = 1.790(5)$ and $\gamma = 1.810(2)$ (measured in white light) and $2V_{\text{meas.}} = 50(10)^\circ$ based on visual estimation from indistinct interference figure; $2V_{\text{calc.}} = 53.6^\circ$. Dispersion, $r < v$, is extreme and becomes manifest in anomalous interference colours. Kenngottite exhibits the following pleochroism: *X* brown-yellow, *Y* blue-green, *Z* olive-brown; $X < Z < Y$. Orientation could not be determined because of indistinct shape and poor quality of crystals. The Gladstone–Dale compatibility index $1 - (K_p/K_c)$ is 0.063 (“fair”) based upon the empirical formula, the density calculated using the single-crystal unit-cell and the measured indices of refraction (Mandarino, 1981). The fair compatibility probably reflects the fine-scale porosity which leads to lower-than-expected indices of refraction.

4. Chemical composition

Samples of kenngottite were analyzed with a Cameca SX-100 electron microprobe operating in the wavelength-dispersive mode with an accelerating voltage of 15 kV, a specimen current of 10 nA and a defocussed beam diameter of 5 μm . The following lines and standards were used: $K\alpha$, hematite (Fe), sanidine (Al, Si), fluorapatite (P, Ca), ZnO (Zn), albite (Na), rhodonite (Mn); $L\alpha$, clinoclase (As). Counting times on peak were 20 s for main elements and 60 s for minor elements, half of these values on each background. The raw intensities were converted to the concentrations using the *PAP* (Pouchou & Pichoir, 1985) matrix-correction software. Checks for F gave no measurable values above background. Water could not be analysed directly because of the minute amount of material available, and was calculated on the basis of 16 O plus 8 (H₂O + OH) groups, taking into account charge balance, from the



Fig. 1. Photomicrograph of brown kennngottite aggregates in cavity of rockbridgeite-group minerals. Field of view 0.8 mm; photo J. Sejkora.

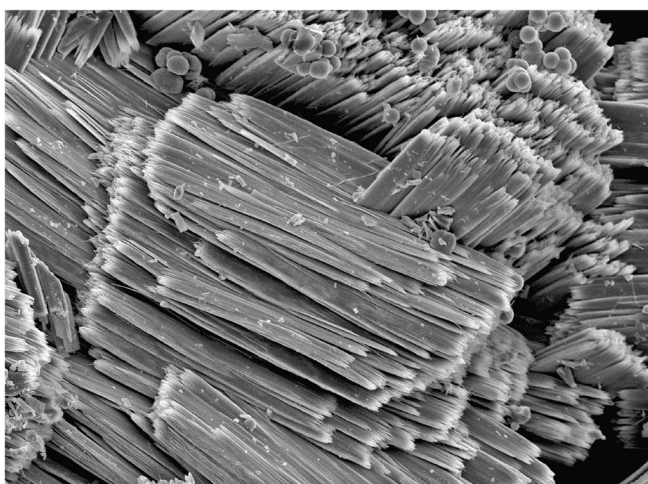


Fig. 2. Aggregates of kennngottite crystals, Krásno. Field of view 1800 μm ; Back-scattered electron image, J. Sejkora and J. Plášil.

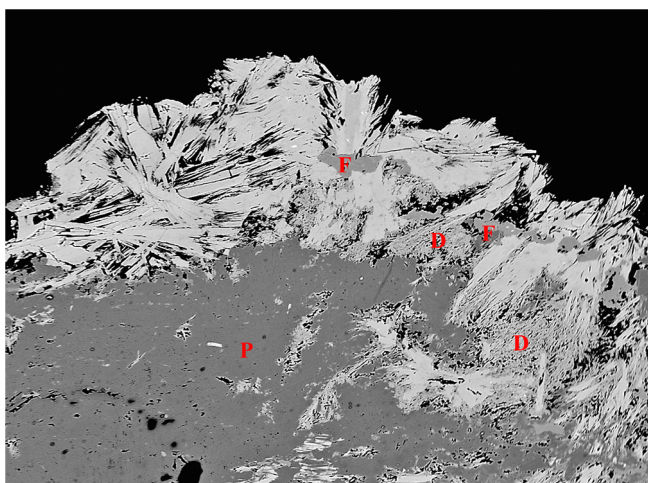


Fig. 3. Back-scattered electron image showing lath-like crystals of kennngottite (light grey) with phosphosiderite (P), fluorapatite grains (F) and finely fibrous Mn-rich dufrénite (D). Field of view 500 μm ; picture J. Sejkora and R. Škoda.

Table 1. Chemical composition of kennngottite from Krásno (wt%).

| Oxide | Mean of 12 analyses | Range | SD |
|--------------------------------|---------------------|-------------|------|
| Na ₂ O | 0.03 | 0–0.13 | 0.05 |
| MnO | 17.82 | 14.42–20.74 | 1.94 |
| CaO | 0.31 | 0.11–0.87 | 0.24 |
| ZnO | 0.32 | 0.16–0.45 | 0.09 |
| Fe ₂ O ₃ | 35.30 | 31.67–38.89 | 2.14 |
| Al ₂ O ₃ | 2.71 | 1.79–3.83 | 0.57 |
| SiO ₂ | 0.08 | 0–0.52 | 0.15 |
| As ₂ O ₅ | 0.15 | 0–0.44 | 0.15 |
| P ₂ O ₅ | 30.80 | 30.13–31.57 | 0.41 |
| H ₂ O* | 9.6 | | |
| Total | 97.12 | | |

*Calculated on the basis of 16 O plus 8 (H₂O + OH) groups with charge balance, from the crystal-structure analysis. All iron is reported as Fe³⁺ based on the structure analysis.

crystal-structure analysis. All iron is reported as Fe³⁺ based on the bond-valence calculations (see below).

Table 1 gives the chemical composition of the kennngottite holotype sample from Krásno (mean of twelve determinations). The results of the chemical analyses correspond with the ideal formula $\text{Mn}_3^{2+}\text{Fe}_4^{3+}(\text{PO}_4)_4(\text{OH})_6(\text{H}_2\text{O})_2$, in which dominant Mn²⁺ in the two non-equivalent Mn sites is partly substituted by Fe³⁺ (up to 1.1 *apfu* – Fig. 4) and, in the three Fe sites, prevailing Fe³⁺ by Al (up to 0.7 *apfu* – Fig. 5). Minor contents of other elements (Zn, Ca, Na) do not exceed 0.04–0.14 *apfu*. In the tetrahedrally coordinated site, only minor Si (up to 0.08 *apfu*) and As (up to 0.03 *apfu*) substitute for P. The empirical formula, normalised to 24 O atoms, is $\text{Mn}_{2.29}^{2+}\text{Ca}_{0.05}\text{Zn}_{0.04}\text{Na}_{0.01}\text{Fe}_{4.04}^{3+}\text{Al}_{0.49}\text{P}_{3.96}\text{As}_{0.01}\text{Si}_{0.01}\text{O}_{24}\text{H}_{9.73}$. The structural formula is $(\text{Mn}_{2.29}\text{Fe}_{0.53}\text{Ca}_{0.05}\text{Zn}_{0.04}\text{Na}_{0.01})_{\Sigma 2.92}(\text{Fe}_{3.51}\text{Al}_{0.49})_{\Sigma 4.00}[(\text{PO}_4)_{3.96}(\text{AsO}_4)_{0.01}(\text{SiO}_4)_{0.01}]_{\Sigma 3.98}(\text{OH})_{6.42}(\text{H}_2\text{O})_{1.66}$. The simplified structural formula is $(\text{Mn}_{2.5}^{2+}\text{Fe}_{0.5}^{3+})\text{Fe}_4^{3+}(\text{PO}_4)_4(\text{OH})_{6.5}(\text{H}_2\text{O})_{1.5}$. The ideal end-member formula is $\text{Mn}_3^{2+}\text{Fe}_4^{3+}(\text{PO}_4)_4(\text{OH})_6(\text{H}_2\text{O})_2$ which requires MnO 23.49, Fe₂O₃ 35.24, P₂O₅ 31.33, H₂O 9.94, total 100.00 wt%.

5. Raman spectroscopy

Kennngottite was investigated with a DXR dispersive Raman Spectrometer (Thermo Scientific) mounted on a confocal Olympus microscope. The Raman signal was excited by a green 532 nm diode-pumped solid-state laser and detected by a CCD detector. The experimental parameters were: 50 \times objective, 10 s exposure time, 100 exposures, 400 lines/mm grating, 25 μm pinhole spectrograph aperture and 6 mW laser power level. Spectra were recorded between 30 and 4200 cm^{-1} (Fig. 6). The instrument was set up by a software-controlled calibration procedure using multiple neon emission lines (wavelength calibration), multiple polystyrene Raman bands (laser frequency calibration) and standardized white-light sources (intensity calibration). Spectral manipulations were performed using the Omnic 9 software (Thermo Scientific).

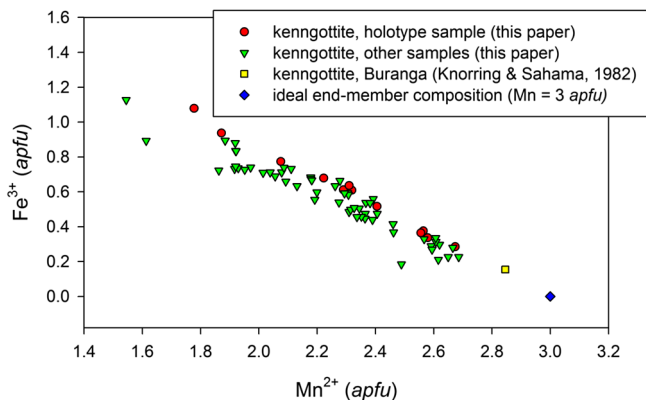


Fig. 4. A plot of Fe^{3+} vs. Mn contents at Mn1 + Mn2 sites of kenngottite.

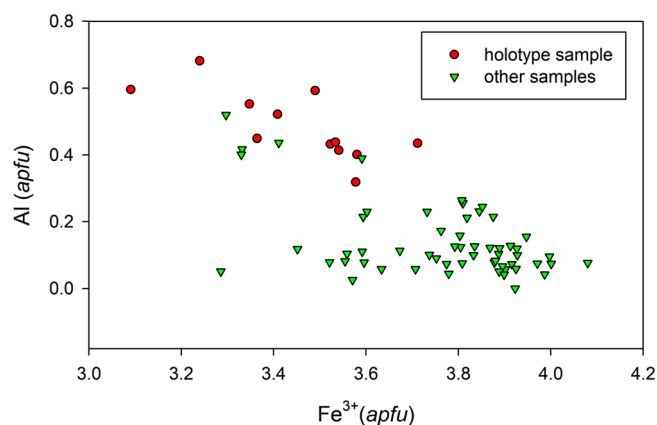


Fig. 5. A plot of Fe^{3+} vs. Al contents at Fe1 + Fe2ab + Fe3ab sites of kenngottite.

The main bands observed are (in wavenumbers): 3570, 3374, 1579, 1101, 1056, 994, 963, 691, 612, 575, 451, 373, 317, 288, 260, 235, 174, 144, 112, 84, 81 and 46 cm^{-1} . The dominant bands in the $1200\text{--}800\text{ cm}^{-1}$ region can be assigned to stretching vibrations of (PO_4) groups (bands at 1101 and 1056 cm^{-1} to ν_3 antisymmetric stretching and those at 994 and 963 cm^{-1} to ν_1 symmetric stretching vibrations). The ν_4 (PO_4) bending vibrations are connected with the bands at 691, 612 and 575 cm^{-1} , and the ν_2 (PO_4) bending vibration with the band at 451 cm^{-1} . The bands 373, 317, 288, 260 and 235 cm^{-1} may be related to the metal-oxygen stretching vibrations (Elliott *et al.*, 2009; Frost *et al.*, 2013; Sejkora *et al.*, 2016). The bands below 200 cm^{-1} are attributed to lattice modes. A broad OH-stretching band running from 3800 to 2800 cm^{-1} with a maximum at 3374 cm^{-1} and a sharp band at 3570 cm^{-1} is assigned to the vibration of (OH) groups. A weak, broad band at 1579 cm^{-1} is connected with ν_2 (δ) bending vibrations of water molecules.

6. X-ray powder diffraction

Powder X-ray diffraction data for kenngottite were obtained using a Rigaku R-Axis Rapid II curved-imaging-plate

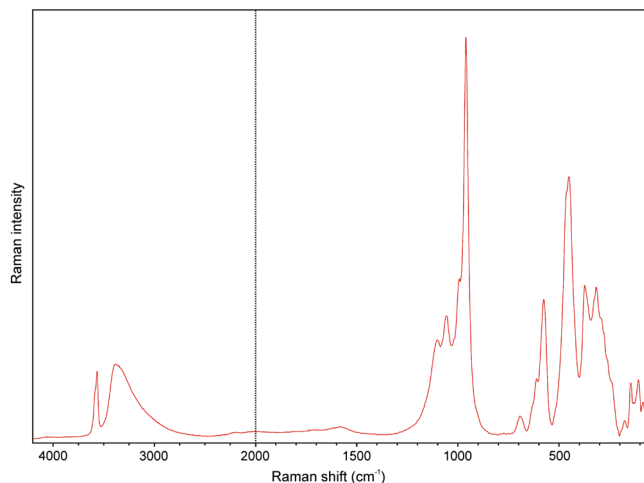


Fig. 6. Raman spectrum of kenngottite (split at 2000 cm^{-1}).

microdiffractometer, with monochromatised $\text{MoK}\alpha$ radiation (50 kV, 40 mA). A Gandolfi-like motion on the ϕ and ω axes was used to randomise the sample. Observed d values and intensities were derived by profile fitting using JADE 2010 software (Materials Data, Inc.). Data (in \AA for $\text{MoK}\alpha$) are given in Table 2. Unit-cell parameters of kenngottite refined from the powder data using JADE 2010 with whole-pattern fitting are: $a = 13.919(9)$, $b = 5.180(9)$, $c = 12.159(10)\text{ \AA}$, $\beta = 98.905(14)^\circ$ and $V = 866.1(18)\text{ \AA}^3$.

7. Single-crystal X-ray diffraction

A thin blade of kenngottite ($0.09 \times 0.04 \times 0.02\text{ mm}$) was used for a data collection on a Rigaku R-Axis Rapid II curved-imaging-plate microdiffractometer utilising monochromatised $\text{MoK}\alpha$ radiation (50 kV, 40 mA). Kenngottite presented particular difficulties for crystal structure analysis due to the irregular intergrowth (Fig. 3) and poor diffracting quality of the fibrous crystals, giving diffuse reflections and strong streaking of the spots. Many crystals were inspected before one was found that gave indexable single-crystal patterns. It was indexed with a primitive monoclinic cell with the parameters reported in Table 3. The data resolution was limited to 1.2 \AA , but it was adequate to obtain a structure solution using *SIR2011* (Burla *et al.*, 2012) in space group $P2_1/a$. During the course of the structure refinement, it was found that two metal atoms, Fe2 and Fe3 were each distributed over two sites (Fe2a/Fe2b and Fe3a/Fe3b, respectively), and an anion coordinated to these atoms, O12, was similarly split into two sites (O12a and O12b). The occupancies of the atom pairs were allowed to refine independently. The structure was refined using JANA2006 (Petříček *et al.*, 2014), with anisotropic displacement parameters for the metal atoms and isotropic displacement parameters for the anions (hydrogen atoms could not be located). The refinement converged to $wR_{\text{obs}} = 0.088$ for 350 reflections with $I > 2\sigma(I)$. Further details of the data collection and crystal-structure refinement are given in Table 3.

Table 2. Powder X-ray diffraction data (*d* in Å) for kennngottite. Note that the calculated intensities have been scaled such that the total of the intensities of the lines contributing to the strongest observed line is 100. Only calculated lines with *I* ≥ 2 are included.

| <i>I</i> _{obs} | <i>d</i> _{obs} | <i>d</i> _{calc} | <i>I</i> _{calc} | <i>hkl</i> | <i>I</i> _{obs} | <i>d</i> _{obs} | <i>d</i> _{calc} | <i>I</i> _{calc} | <i>hkl</i> |
|-------------------------|-------------------------|--------------------------|--------------------------|------------|-------------------------|-------------------------|--------------------------|--------------------------|------------|
| 8 | 12.04 | 12.0133 | 7 | 0 0 1 | 2 | 2.306 | 2.2933 | 2 | 2 2 2 |
| 22 | 6.90 | 6.8711 | 23 | 2 0 0 | 6 | 2.2167 | 2.2147 | 4 | 5 1 3 |
| | | 6.4058 | 4 | 2 0 1 | 8 | 2.1620 | 2.1662 | 3 | 2 0 5 |
| 26 | 5.16 | 5.1860 | 18 | 0 1 0 | 4 | 2.1345 | 2.1410 | 3 | 3 1 4 |
| 47 | 4.87 | { 4.9137 | 3 | 2 0 2 | 13 | 2.1180 | { 2.1152 | 2 | 6 1 1 |
| | | 4.8520 | 18 | 1 1 0 | | | 2.1079 | 7 | 1 1 5 |
| 6 | 4.56 | 4.5866 | 4 | 1 1 1 | 13 | 2.0811 | { 2.0721 | 9 | 4 2 1 |
| 8 | 4.40 | 4.4161 | 7 | 1 1 1 | | | 2.0697 | 3 | 4 2 0 |
| 18 | 4.194 | { 4.2116 | 9 | 2 0 2 | 24 | 2.0362 | { 2.0285 | 5 | 5 1 4 |
| | | 4.1393 | 14 | 2 1 0 | | | 2.0266 | 11 | 2 2 3 |
| 8 | 4.056 | 4.0307 | 3 | 2 1 1 | 6 | 1.9763 | 1.9741 | 3 | 6 0 4 |
| 3 | 3.961 | 4.0044 | 9 | 0 0 3 | 28 | 1.9506 | { 1.9627 | 5 | 0 2 4 |
| | | 3.8792 | 5 | 1 1 2 | | | 1.9396 | 18 | 2 2 4 |
| 10 | 3.727 | 3.7185 | 9 | 2 0 3 | | | 1.9126 | 2 | 4 2 3 |
| | | 3.6777 | 7 | 1 1 2 | 12 | 1.8541 | 1.8554 | 4 | 7 1 1 |
| 89 | 3.458 | { 3.4468 | 15 | 4 0 1 | | | 1.8400 | 2 | 4 0 5 |
| | | 3.4332 | 68 | 3 1 0 | | | 1.8389 | 3 | 2 2 4 |
| 100 | 3.209 | { 3.2485 | 18 | 2 0 3 | 7 | 1.7810 | 1.7738 | 6 | 5 1 4 |
| | | 3.2046 | 48 | 3 1 1 | 14 | 1.7378 | { 1.7385 | 6 | 8 0 1 |
| | | 3.1745 | 2 | 1 1 3 | | | 1.7276 | 2 | 6 2 1 |
| | | 3.1695 | 3 | 0 1 3 | 14 | 1.7179 | 1.7162 | 8 | 0 0 7 |
| | | 3.1414 | 28 | 3 1 2 | | | 1.7034 | 2 | 6 2 2 |
| 31 | 3.023 | { 3.0090 | 21 | 1 1 3 | 16 | 1.6751 | { 1.6725 | 3 | 6 2 1 |
| | | 3.0033 | 6 | 0 0 4 | | | 1.6624 | 2 | 2 2 5 |
| | | 2.9225 | 2 | 2 0 4 | | | 1.6600 | 2 | 5 1 6 |
| 7 | 2.876 | { 2.8706 | 6 | 4 1 1 | 16 | 1.6494 | { 1.6483 | 2 | 6 2 3 |
| | | 2.8641 | 3 | 4 1 0 | | | 1.6398 | 2 | 4 0 7 |
| 6 | 2.809 | 2.8017 | 4 | 4 0 2 | 18 | 1.6228 | { 1.6242 | 5 | 4 0 6 |
| | | 2.7530 | 2 | 2 1 3 | | | 1.6173 | 3 | 3 3 0 |
| 46 | 2.623 | { 2.6183 | 29 | 1 1 4 | 27 | 1.5995 | { 1.6023 | 7 | 6 2 2 |
| | | 2.6081 | 2 | 2 0 4 | | | 1.6015 | 2 | 8 0 4 |
| | | 2.5930 | 12 | 0 2 0 | | | 1.5914 | 2 | 3 3 1 |
| 13 | 2.490 | 2.4936 | 5 | 1 1 4 | | | 1.5880 | 3 | 8 0 2 |
| 11 | 2.457 | { 2.4691 | 5 | 3 1 3 | 34 | 1.5772 | 1.5707 | 17 | 6 2 4 |
| | | 2.4569 | 4 | 4 0 4 | 23 | 1.5206 | 1.5155 | 6 | 6 2 3 |
| | | 2.4460 | 7 | 5 1 1 | 12 | 1.4954 | { 1.5045 | 3 | 2 2 6 |
| 49 | 2.429 | { 2.4285 | 11 | 5 1 0 | | | 1.5019 | 2 | 1 3 4 |
| | | 2.4260 | 13 | 2 2 0 | 25 | 1.4679 | { 1.4633 | 2 | 5 3 0 |
| | | 2.4024 | 17 | 3 1 4 | | | 1.4612 | 2 | 4 0 8 |
| | | 2.3856 | 2 | 2 0 5 | 11 | 1.4469 | 1.4571 | 4 | 1 1 8 |

Refined atom coordinates, equivalent isotropic displacement parameters and bond-valence sums (BVSs, Gagné & Hawthorne, 2015) for kennngottite are given in Table 4 and polyhedral bond distances in Table 5. The BVS values are consistent with trivalent cations ordered in Fe1 to Fe3 and predominantly divalent cations ordered in Mn1 and Mn2. Good agreement with mean bond distances and BVS values was obtained on the basis that the minor Fe in the Mn1 and Mn2 sites was Fe³⁺, with the Mn being divalent. The M–O mean distances for Fe1 and Fe2a sites are shorter than expected for Fe³⁺, consistent with minor Al also occupying these sites. The low BVSs for O9 to O12 are consistent with these being predominantly OH⁻. Charge balance in the simplified formula for kennngottite, (Mn_{2.5}Fe_{0.5}³⁺)Fe₄³⁺(PO₄)₄(OH)_{6.5}(H₂O)_{1.5}, requires 1.5 H₂O *pfu* and from the BVS values in Table 4, these are most likely distributed over the O10, O11 and O12b sites.

A projection of the structure of kennngottite along [010] is shown in Fig. 7. It contains Mn2–Fe1–Mn2-centred *h*-clusters (Moore, 1970) of face-shared octahedra that are linked by edge-sharing with Mn1-centred octahedra to form chains along [001]. The chains are linked by corner-sharing with PO₄ tetrahedra to form layers parallel to (100). These layers alternate along [100] with layers containing the Fe2- and Fe3-centred octahedra. Groups of three corner-connected octahedra, centred by Fe3–Fe2–Fe3, are connected into chains along [001] by corner-sharing with PO₄ tetrahedra. The chains are stacked along [010] as shown in Fig. 8. The Fe2a- and Fe3a-centred octahedra that have ~75% occupancy alternate along [010] with Fe2b- and Fe3b-centred octahedra that have ~25% occupancy.

Kennngottite has the same stoichiometry as souzalite, (Mg,Fe²⁺)₃(Al,Fe³⁺)₄(PO₄)₄(OH)₆(H₂O)₂ (Le Bail *et al.*, 2003), with Mn²⁺ replacing Mg and Fe³⁺ replacing Al.

Table 3. Crystal data and structure refinement details for kenngottite.

| | |
|---|---|
| Simplified formula | (Mn _{2.5} ²⁺ Fe _{0.5} ³⁺)Fe ₄ ³⁺ (PO ₄) ₄ (OH) _{6.5} (H ₂ O) _{1.5} |
| Temperature | 293(2) K |
| Wavelength | 0.7107 Å |
| Space group | <i>P2/a</i> |
| Unit-cell parameters | <i>a</i> = 13.909(10) Å <i>b</i> = 5.186(4) Å <i>c</i> = 12.159(9) Å β = 98.880(10)° |
| Volume | 866.5(11) Å ³ |
| Z | 2 |
| Absorption coefficient | 5.87 mm ⁻¹ |
| Crystal size | 0.09 × 0.04 × 0.02 mm ³ |
| θ range for data collection | 3.0–17.2° |
| Index ranges | $\bar{1}1 \leq h \leq 11$, $\bar{4}, \leq k \leq 4$, $\bar{1}0 \leq l \leq 10$ |
| Reflections collected | 4711 |
| Independent reflections | 517 [<i>R</i> _{int} = 0.18] |
| Reflections with <i>I</i> _o > 3σ(<i>I</i>) | 350 |
| Completeness to 17.2° | 99.0% |
| Refinement method | Full-matrix least-squares on <i>F</i> ² |
| Constraints/restraints/parameters | 13/0/113 |
| Goodness-of-fit on <i>F</i> ² | 1.96 |
| Final <i>R</i> indices [<i>I</i> > 2σ(<i>I</i>)] | <i>R</i> _{obs} = 0.089, <i>wR</i> _{obs} = 0.087 |
| <i>R</i> indices (all data) | <i>R</i> _{obs} = 0.135, <i>wR</i> _{obs} = 0.091 |
| Largest diff. peak and hole | 0.94 and −1.13 e Å ⁻³ |

Table 4. Refined atom coordinates, equivalent (Fe, Mn and P sites) or isotropic (O sites) displacement parameters (Å²) and bond valence sum (BVS) values for kenngottite.

| | <i>x</i> | <i>y</i> | <i>z</i> | <i>U</i> _{eq} | BVS |
|-------|------------|------------|-------------|------------------------|------|
| Fe1 | 0.25 | 0.2408(16) | 0.5 | 0.064(3) | 3.23 |
| Fe2a* | 0.5 | 0.5 | 0 | 0.062(5) | 3.35 |
| Fe2b* | 0.5 | 1 | 0 | 0.062(5) | 2.65 |
| Fe3a* | 0.5453(5) | 0.4764(14) | 0.3060(6) | 0.054(3) | 3.11 |
| Fe3b* | 0.4539(17) | 0.996(5) | 0.691(2) | 0.054(3) | 2.50 |
| Mn1 | 0.25 | 0.2593(16) | 1 | 0.055(3) | 2.16 |
| Mn2 | 0.2138(4) | 0.2536(11) | 0.7260(4) | 0.059(3) | 2.19 |
| P1 | 0.3155(7) | 0.748(2) | 0.8564(8) | 0.055(4) | 5.09 |
| P2 | 0.3831(7) | 0.737(2) | 0.4409(8) | 0.061(5) | 5.17 |
| O1 | 0.3915(14) | 0.749(4) | 0.9564(15) | 0.048(6) | 1.95 |
| O2 | 0.3589(13) | 0.752(4) | 0.7481(15) | 0.047(6) | 1.82 |
| O3 | 0.2553(14) | 0.998(5) | 0.8604(16) | 0.056(7) | 1.97 |
| O4 | 0.2460(15) | 0.511(5) | 0.8598(18) | 0.067(7) | 1.96 |
| O5 | 0.4340(14) | 0.724(4) | 0.5572(17) | 0.058(6) | 1.98 |
| O6 | 0.3182(13) | 0.981(4) | 0.4205(15) | 0.045(6) | 2.04 |
| O7 | 0.4523(15) | 0.744(4) | 0.3524(16) | 0.064(6) | 1.69 |
| O8 | 0.3138(14) | 0.511(5) | 0.4164(16) | 0.056(7) | 2.17 |
| O9 | 0.3435(13) | 0.248(4) | 0.6392(14) | 0.046(6) | 1.26 |
| O10 | 0.4343(15) | 0.229(5) | 0.2558(16) | 0.073(7) | 0.91 |
| O11 | 0.5926(12) | 0.759(4) | −0.0423(14) | 0.044(6) | 0.92 |
| O12a* | 0.516(3) | 0.582(11) | 0.155(4) | 0.078(17) | 1.30 |
| O12b* | 0.516(4) | 0.75(2) | 0.159(5) | 0.078(17) | 0.66 |

*Site occupancies: Fe2a/Fe2b = 0.75(2)/0.20(1); Fe3a/Fe3b = 0.75(1)/0.201(8); O12a/O12b = 0.68(7)/0.36(6).

The structures of the two minerals are closely related. Souzalite has triclinic symmetry with *a* = 7.222, *b* = 11.780, *c* = 5.117 Å, α = 90.16, β = 109.94, γ = 81.33°. The triclinic cell for souzalite is related to the

Table 5. Polyhedral bond distances (Å) for kenngottite.

| | | | |
|---------------|---------|---------------|---------|
| Fe1–O6 × 2 | 1.98(2) | | |
| Fe1–O8 × 2 | 2.02(2) | | |
| Fe1–O9 × 2 | 1.97(2) | | |
| Av. | 1.99 | | |
| Fe2a–O1 × 2 | 1.99(2) | Fe2b–O1 × 2 | 2.00(2) |
| Fe2a–O11 × 2 | 1.98(2) | Fe2b–O11 × 2 | 1.92(2) |
| Fe2a–O12a × 2 | 1.92(4) | Fe2b–O12b × 2 | 2.31(8) |
| Av. | 1.96 | Av. | 2.08 |
| Fe3a–O2 | 1.97(2) | Fe3b–O2 | 2.03(3) |
| Fe3a–O5 | 1.94(2) | Fe3b–O5 | 2.13(3) |
| Fe3a–O7 | 2.03(2) | Fe3b–O7 | 2.00(3) |
| Fe3a–O9 | 2.14(2) | Fe3b–O9 | 2.04(3) |
| Fe3a–O10 | 2.03(2) | Fe3b–O10 | 1.97(3) |
| Fe3a–O12a | 1.90(4) | Fe3b–O12b | 2.23(9) |
| Av. | 2.00 | Av. | 2.07 |
| Mn1–O3 × 2 | 2.18(2) | Mn2–O3 | 2.12(2) |
| Mn1–O4 × 2 | 2.14(3) | Mn2–O4 | 2.10(2) |
| Mn1–O11 × 2 | 2.17(2) | Mn2–O6 | 2.26(2) |
| Av. | 2.16 | Mn2–O8 | 2.17(2) |
| | | Mn2–O9 | 2.22(2) |
| | | Mn2–O10 | 2.11(2) |
| | | Av. | 2.16 |
| P1–O1 | 1.48(2) | P2–O5 | 1.48(2) |
| P1–O2 | 1.53(2) | P2–O6 | 1.55(2) |
| P1–O3 | 1.55(2) | P2–O7 | 1.55(2) |
| P1–O4 | 1.57(1) | P2–O8 | 1.52(3) |
| Av. | 1.53 | Av. | 1.52 |

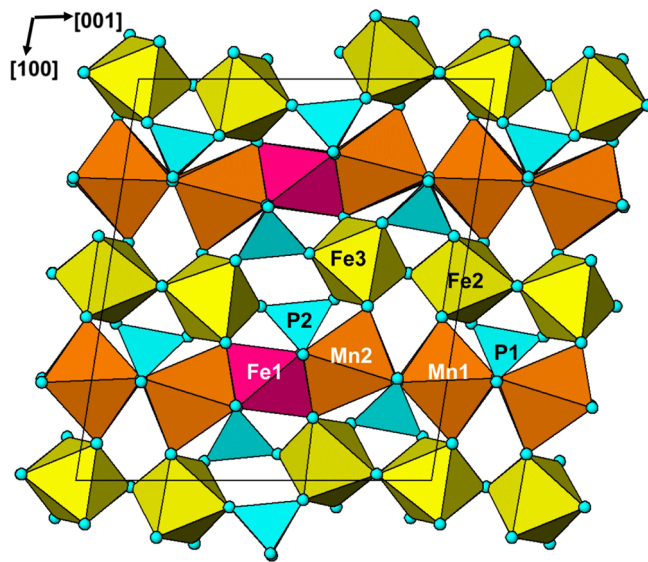


Fig. 7. [010] projection of the crystal structure of kenngottite; only Fe2a- and Fe3a-centred octahedra ("Fe2", "Fe3") are shown for clarity.

monoclinic cell for kenngottite by the transformation (0.5 0.5 0/0 0 $\bar{1}$ /0 $\bar{1}$ 0). The main difference between the two structures is that the [001] chains containing the trimeric clusters of corner-connected *M3*–*M2*–*M3*–centred octahedra (*M* = Fe, Al) lie in (010) planes in kenngottite, but in (110)

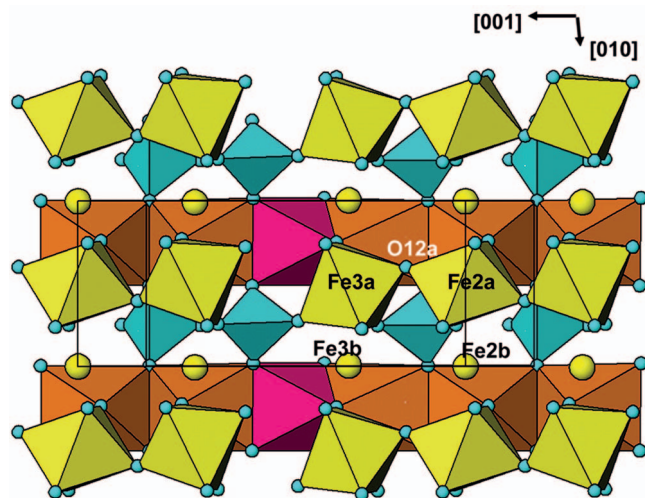


Fig. 8. (100) layer containing trimers of corner-connected Fe2a–Fe3a–Fe2a-centred octahedra. The partially occupied sites Fe2b and Fe3b are shown as spheres.

Table 6. Comparison of kennngottite with souzalite and gormanite.

| | Kennngottite | Souzalite | Gormanite |
|--|--|--|---|
| Reference | This paper | Le Bail <i>et al.</i> (2003), Pecora & Fahey (1949) | Sturman <i>et al.</i> (1981) |
| End-member Formula | $\text{Mn}_3^{2+}\text{Fe}_4^{3+}(\text{PO}_4)_4(\text{OH})_6 \cdot 2\text{H}_2\text{O}$ | $\text{Mg}_3\text{Al}_4(\text{PO}_4)_4(\text{OH})_6 \cdot 2\text{H}_2\text{O}$ | $\text{Fe}_3^{2+}\text{Al}_4(\text{PO}_4)_4(\text{OH})_6 \cdot 2\text{H}_2\text{O}$ |
| Space group | <i>P21a</i> | <i>P-1</i> | <i>P-1</i> or <i>P1</i> |
| <i>a</i> [Å] | 13.909(10) | 7.2223(1) | 11.79(1) |
| <i>b</i> [Å] | 5.186(4) | 11.7801(1) | 5.11(1) |
| <i>c</i> [Å] | 12.159(9) | 5.1169(1) | 13.61(1) |
| α [°] | | 90.158(1) | 90.83(8) |
| β [°] | 98.880(10) | 109.938(1) | 99.00(8) |
| γ [°] | | 81.330(1) | 90.08(8) |
| <i>V</i> [Å ³] | 866.5(11) | 404.02(1) | 809.8 |
| <i>Z</i> | 2 | 1 | 2 |
| <i>d</i> [Å]/ <i>I</i> _{obs.} | 4.87/47 3.458/89 3.209/100 3.023/31 2.623/46 2.429/49 | 5.35/s 3.79/s 2.690/vs 2.472/s 2.027/s | 4.761/60 3.395/100 3.154/60 3.062/40 2.925/80 2.554/90 |
| Density [g cm ⁻³] | 3.421 | 3.087 | 3.13 |
| Optical | Biaxial (+) | Biaxial (–) | Biaxial (–) |
| α | 1.785(5) | 1.618(2) | 1.619(3) |
| β | 1.790(5) | 1.642(2) | 1.653(3) |
| γ | 1.810(5) | 1.652(2) | 1.660(3) |

planes in souzalite (indices relative to the monoclinic cell). The *M2*- and *M3*-centred octahedra in souzalite are fully ordered and alternate with vacant sites along the 5 Å axis, whereas in kennngottite there is a 0.75/0.25 disorder of these sites along the 5 Å axis. In the structurally related mineral rockbridgeite, there is complete disorder of the corner-connected octahedra in successive sites along the 5 Å axis (Moore, 1970).

8. Relation to other species

Kennngottite is structurally related to souzalite $\text{Mg}_3\text{Al}_4(\text{PO}_4)_4(\text{OH})_6 \cdot 2\text{H}_2\text{O}$ (Pecora & Fahey, 1949; Le Bail *et al.*, 2003) and gormanite $\text{Fe}_3\text{Al}_4(\text{PO}_4)_4(\text{OH})_6 \cdot 2\text{H}_2\text{O}$ (Sturman *et al.*, 1981). A comparison of their crystallographic parameters and physical properties is shown in Table 6. Kennngottite is identical with unnamed phase *UNK9* (Sejkora *et al.*, 2006c) and probably also with the unnamed Fe–Mn “dufrénite-like” mineral from Buranga, Rwanda (von Knorring & Sahama, 1982). It is a member of Nickel – Strunz class 8.DC: Phosphates, *etc.* with additional anions, with H_2O ; with only medium-sized cations, (OH, *etc.*): $\text{RO}_4 = 1:1$ and $<2:1$.

Acknowledgements: The authors wish to express their thanks to Radek Škoda (Masaryk University, Brno), Zdeněk Dolníček (National Museum, Prague) and Jakub Plášil (Academy of Sciences of the Czech Republic, Prague) for their kind support in this study. The editor-in-chief Sergey V. Krivovichev, Uwe Kolitsch and an anonymous reviewer are acknowledged for valuable comments and suggestions that helped to improve the manuscript. This work was supported financially by the Ministry of Culture of the Czech Republic (long-term project DKRVO 2019-2023/1. II.a; National Museum, 00023272).

References

- Beran, P. & Sejkora, J. (2006): The Krásno Sn–W ore district near Horní Slavkov: mining history, geological and mineralogical characteristics. *J. Czech Geol. Soc.*, **51**, 3–42.
- Burla, M.C., Caliendo, R., Camalli, M., Carrozzini, B., Cascarano, G.L., Giacovazzo, C., Mallamo, M., Mazzone, A., Polidori, G., Spagna, R. (2012): *SIR2011*: a new package for crystal structure determination and refinement. *J. Appl. Cryst.*, **45**, 357–361.
- Elliott, P., Kolitsch, U., Giester, G., Libowitzky, E., McCammon, C., Pring, A., Birch, W.D., Brugger, J. (2009): Description and crystal structure of a new mineral – plimerite, $\text{ZnFe}_4^{3+}(\text{PO}_4)_3(\text{OH})_5$ – the Zn-analogue of rockbridgeite and frondelite, from Broken Hill, New South Wales, Australia. *Mineral. Mag.*, **73**, 131–148.
- de Fourestier, J. (1999): Glossary of mineral synonyms. The Canadian mineralogist special publication 2. Mineralogical Association of Canada, Ottawa.
- Frost, R.L., Xi, Y., Scholz, R., Belotti, F.M., Beganovic, M. (2013): SEM-EDX, Raman and infrared spectroscopic characterization of the phosphate mineral frondelite (Mn^{2+})(Fe^{3+})₄(PO_4)₃(OH)₅. *Spectrochim. Acta A: Mol. Biomol. Spectrosc.*, **110**, 7–13.
- Gagné, O.C. & Hawthorne, F.C. (2015): Comprehensive derivation of bond-valence parameters for ion pairs involving oxygen. *Acta Crystallogr. B: Struct. Sci. Cryst. Eng. Mater.*, **71**, 562–578.
- Kennngott, A. (1851): Karpolith von Schlaggenwald. in “Berichte über die Mittheilungen von Freunden der Naturwissenschaften in Wien”, W. von Haidinger, ed. **Band VII**.
- von Knorring, O. & Sahama, T.G. (1982): Some FeMn phosphates from the Buranga pegmatite, Rwanda. *Schweiz. Mineral. Petrogr. Mitt.*, **62**, 343–352.
- Le Bail, A., Stephens, P.W., Hubert, F. (2003): A crystal structure for the souzalite/gormanite series from synchrotron powder diffraction data. *Eur. J. Mineral.*, **15**, 719–723.

- Mandarino, J.A. (1981): The Gladstone-Dale relationship: Part IV. The compatibility concept and its application. *Can. Mineral.*, **19**, 441–450.
- Mills, S.J., Kolitsch, U., Birch, W.D., Sejkora, J. (2008): Kunatite, $\text{CuFe}_2^{3+}(\text{PO}_4)_2(\text{OH})_2 \cdot 4\text{H}_2\text{O}$, a new member of the whitmoreite group, from Lake Boga, Victoria, Australia. *Aust. J. Mineral.*, **14**, 3–12.
- Mills, S.J., Kampf, A.R., Sejkora, J., Adams, P.M., Birch, W.D., Plášil, J. (2011): langreyite: a new secondary phosphate mineral closely related to perhamite. *Mineral. Mag.*, **75**, 327–336.
- Mills, S.J., Sejkora, J., Kampf, A.R., Grey, I.E., Bastow, T.J., Ball, N.A., Adams, P.M., Raudsepp, M., Cooper, M.A. (2012): Krásnoite, the fluorophosphate analogue of perhamite, from the Huber open pit, Czech Republic and the Silver Coin mine, Nevada, USA. *Mineral. Mag.*, **76**, 625–634.
- Moore, P.B. (1970): Crystal chemistry of the basic iron phosphates. *J. Appl. Cryst.*, **55**, 135–169.
- Palache, C., Berman H., Frondel, C. (1944): The system of mineralogy of James Dwight Dana and Edward Salisbury Dana Yale University 1837–1892. in “Volume I: Elements, Sulfides, Sulfosalts, Oxides”, 7th edition, John Wiley and Sons, Inc, New York, NY. Revised and enlarged: 424.
- Pecora, W.T. & Fahey, J.J. (1949): The Corrego Frio pegmatite, Minas Gerais: scorzalite and souzalite, two new phosphate minerals. *Am. Mineral.*, **34**, 83–93.
- Petříček, V., Dušek, M., Palatinus, L. (2014): Crystallographic computing system JANA2006: general features. *Zeit. Kristallogr.*, **229**, 345–352.
- Pouchou, J.L. & Pichoir, F. (1985): “PAP” (ϕ ρ Z) procedure for improved quantitative microanalysis. in “Microbeam analysis”, J.T. Armstrong, ed. San Francisco Press, San Francisco, California, 104–106.
- Sejkora, J., Ondruš, P., Fikar, M., Veselovský, F., Mach, Z., Gabašová, A., Škoda, R., Beran, P. (2006a): Supergene minerals at the Huber stock and Schnöd stock deposits, Krásno ore district, the Slavkovský les area, Czech Republic. *J. Czech Geol. Soc.*, **51**, 57–101.
- Sejkora, J., Škoda, R., Ondruš, P., Beran, P., Süsner, C. (2006b): Mineralogy of phosphate accumulations in the Huber stock, Krásno ore district, Slavkovský les area, Czech Republic. *J. Czech Geol. Soc.*, **51**, 103–147.
- Sejkora, J., Škoda, R., Ondruš, P. (2006c): New naturally occurring mineral phases from the Krásno – Horní Slavkov area, western Bohemia, Czech Republic. *J. Czech Geol. Soc.*, **51**, 159–187.
- Sejkora, J., Plášil, J., Filip, J. (2011): Plimerite from Krásno near Horní Slavkov ore district, Czech Republic. *J. Geosci.*, **56**, 215–229.
- Sejkora, J., Grey, I.E., Kampf, A.R., Price, J.R., Čejka, J. (2016): Tvrdýite, $\text{Fe}^{2+}\text{Fe}_3^{2+}\text{Al}_3(\text{PO}_4)_4(\text{OH})_5(\text{OH}_2)_4 \cdot 2\text{H}_2\text{O}$, a new phosphate mineral from Krásno near Horní Slavkov, Czech Republic. *Mineral. Mag.*, **80**, 1077–1088.
- Sturman, B.D., Mandarino, J.A., Mrose, M.E., Dunn, P.J. (1981): Gormanite, $\text{Fe}_3^{2+}\text{Al}_4(\text{PO}_4)_4(\text{OH})_6 \cdot 2\text{H}_2\text{O}$, the ferrous analogue of souzalite, and new data for souzalite. *Can. Mineral.*, **19**, 381–387.

Received 1 February 2019

Modified version received 20 March 2019

Accepted 21 March 2019